The Use of UV-visible Spectroscopy to Measure the Band Gap of a Semiconductor

Zhebo Chen and Thomas F. Jaramillo
Department of Chemical Engineering, Stanford University
Edited by Bruce Brunschwig 09/19/2017

Section 1: Introduction to UV-Vis spectroscopy

In ultraviolet-visible light (UV-vis) spectroscopic, light absorption is measured as a function of wavelength. The spectrum provides information about electronic transitions occurring in the material. The Beer-Lambert law states that the Transmittance, *i.e.*, the light transmitted (I_T) over the incident intensity (I_0), is dependent on the path length of the light through the sample (l), the absorption cross section (σ) of the sample's transition, and the difference in the population of the initial state (N_1) and final state (N_2), Equation 1.1.

$$T = \frac{I_T}{I_o} = \exp(-\sigma(N_1 - N_2)l \tag{1.1}$$

This is often written in a form referred to as Beer's Law, equation 1.2

$$A = \varepsilon cl = -\log_{10}\left(\frac{I_T}{I_0}\right) \text{ or } I_T = I_0 10^{-\varepsilon cl} \tag{1.2}$$

where A, is the absorbance, ε is the molar absorptivity coefficient of the material, c is the concentration of the absorbing species, and l is the path length of the light through the sample.

The absorbance A can be normalized to the path length l of the light through the material (e.g., the thickness of a film), producing the absorption coefficient α[1]

$$\alpha(\text{cm}^{-1}) = \frac{\ln(10) \times A}{l(\text{cm})} = \ln(10)\varepsilon c \tag{1.3}$$

$$\alpha l = -\ln\left(\frac{I_{\mathrm{T}}}{I_0}\right) \text{ or } I_{\mathrm{T}} = I_0 \exp(-\alpha l) \tag{1.4}$$

The "efficiency" of the photon absorption process occurring within a sample, formally known as absorptance, f_{A} (this is different from absorbance), is defined as the fraction of photons absorbed per photons impinging on the sample assuming there is no reflection from the sample (see below Eq 1.7) where I_{abs} is the light absorbed.

$$f_A = \frac{\mathrm{I}_0 - I_T}{I_0} = 1 - T = \frac{I_{abs}}{I_0} = 1 - 10^{-A} \tag{1.5}$$

For semiconductors, UV-vis spectroscopy offers a convenient method of estimating the optical band gap, since it probes electronic transitions between the valence band and the conduction band. The optical band gap is not necessarily equal to the electronic band gap, which is defined as the energy difference between the valence band minimum (VBM) and the conduction band maximum (CBM); however, it is often approximated as such because there are few convenient methods for measuring the electronic band gap. Exciton binding energies, d-d transitions, phonon absorption and emissions, and excitations to or from defect bands and color centers can complicate interpretation of UV-vis spectra; nevertheless, an estimation of the optical band gap is obtainable. Furthermore, UV-vis allows for the characterization of this electronic transition as either direct or indirect and whether it is allowed or forbidden.

A *direct transition* is described as a two-particle interaction between an electron and a photon, whereas an *indirect transition* is described as a three-particle interaction (photon, electron, phonon) to ensure momentum conservation. A transition is *allowed* or *forbidden* depending on the dipole selection rules associated with the system. The shape of the UV-vis absorption spectrum can distinguish between these transitions.

Section 2: Limitations of UV-vis spectroscopy

The UV-vis measurement is relatively straightforward, and the data obtained is highly reproducible from lab to lab despite differences in lamp sources, spectrometers, experimental configuration, etc. However, to derive a band gap value from a UV-vis measurement, the data must be interpreted. Interpretation is often made difficult by the shape of the absorption spectrum and the ability of the user to estimate the line tangent to

the slope of the absorption data. This procedure requires the drawing of a tangent line to the curve, which is subjective and can result in significant error. The absorption edge in many materials is characterized by an exponential tail with values of $\alpha < \sim 10^4$ cm^{-1}.[2, 3] Fitting a tangent to a point within this tail will underestimate the band gap of the material, as seen in Figure 1.

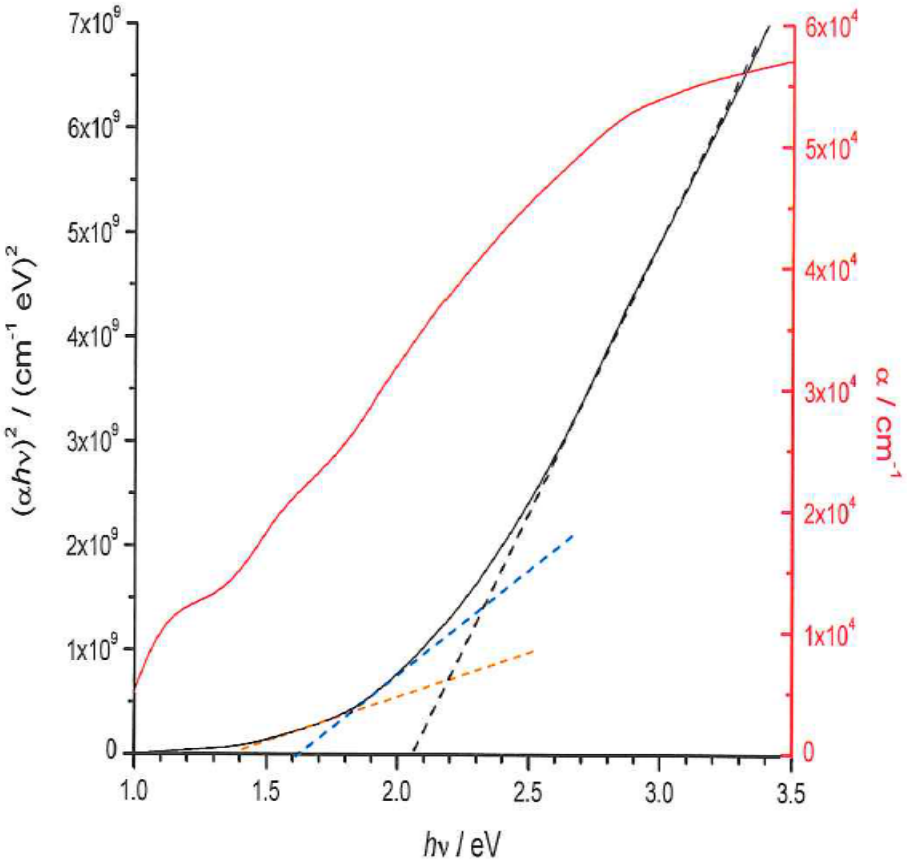

Figure 1 Direct (allowed) band gap Tauc plot (solid black) and absorption coefficient (solid red) plot of MoS_2. Extrapolation of $(\alpha h\nu)^2$ to the x-intercept using the low energy exponential tail region results in an underestimate of the band gap (dashed blue and dashed orange). In this case, the correct trend line {dashed black) is drawn when fitted to values of $\alpha > 4.5 \times 10^4$ cm^{-1}.

Damage to the working sample does not typically occur in UV-vis spectroscopic measurements unless the lamp exhibits particularly intense irradiation in the infrared that could locally heat the sample. The user can correct for this by using a water jacket to attenuate the intensity of these peaks. The possibility of degradation from high energy UV radiation also exists, which can be particularly problematic in samples involving organics.

Other sources of error in a UV-vis measurement often arise from reflection, refraction, or scattering that may occur at the surface and interfaces of the material or from the unwanted transmission of light during a diffuse reflectance experiment. These effects decrease the amount of light that reaches the detector and produce seemingly higher absorption values. This can result in nonzero baselines or sloped base lines that need to be considered when analyzing spectra. To minimize reflection or refraction during a transmission experiment, the user should ensure that the sample sits normal to the path of incident light. Scattering effects can be minimized by placing the sample as close as possible to the detector. In a diffuse reflectance measurement, the user should place a highly reflective standard against a transparent sample to decrease transmitted light.

Pitfalls of the experimental procedure often come from an improperly positioned sample, as mentioned above, or from measurements performed before the lamp has had proper time to warm up, resulting in an unreliable base line. Improper shielding of the sampling chamber from ambient lighting can also contribute to the background signal and decrease the signal-to-noise ratio. Lastly, harmonics that arise from using a grating monochromator can lead to inaccurate measurements if they are not removed using long-pass-filters.

Section 3: Experiment methods for UV-vis spectroscopic measurements

The two most used UV-vis configurations are transmission and diffuse reflectance, each of which will be further discussed in detail. Both techniques follow the general experimental format:

- Turn on lamp source and allow at least 15 minutes for lamp to warm up
- Place reference sample into the light path
- Collect a baseline of the reference sample and, if available, a dark scan
- Place working sample into the light path
- Collect transmission/reflection spectrum of working sample
- Calculate the absorption coefficient and convert wavelength in nm to eV
- Fit the spectrum to estimate the band gap and assess whether it is direct or indirect and whether it is forbidden or allowed

There is little preparation time involved in a UV-vis spectroscopic measurement other than the effort required to place the sample in a proper sample holder for the instrument. The amount of time required to conduct the experiment is minimal and mostly determined by the time required for the lamp to warm up. Sampling time will vary depending on the speed and range of the scan but generally takes no more than a few minutes. Analysis time is similarly short, requiring no more than a few minutes to plot and analyze the data in a program.

Section 3.2: Experimental Parameters

The experimentalist must first decide between using a transmission or diffuse reflectance configuration. In general, transmission mode is used for transparent samples. Often these materials are single crystals or thin films supported on transparent glass substrates. Opaque or translucent samples, such as materials supported on metallic substrates or solids made up on small particles or multiple small crystals, cannot be used since they strongly scatter light and in transmission mode the spectrometer would indicate complete absorption across all wavelengths of light. As such, opaque samples must utilize a diffuse reflectance configuration. However, a diffuse reflectance configuration can also be used for transparent samples if a reflectance standard is placed behind the sample to reflect all transmitted light back through the sample and into the integrating sphere as shown in Figure 5.

It is beneficial to utilize the full wavelength range of the UV-vis spectrometer to measure a more reliable baseline and absorption plateau. Because the sampling time is typically short, choosing a smaller range does not provide a significant decrease in the time required to perform the measurement. However, two situations may arise that require a decreased range of measurement. If the sample is particularly sensitive to local heating from absorbing infrared radiation, then it may be beneficial to limit the spectrometer to wavelengths below -800 nm. If the sample degrades from high energy UV radiation, then limiting wavelengths to above - 400 nm may be required, although the exact cut-off is dependent on the material.

Section 3.3: Transmission UV-vis.

In transmission configuration, the user places the sample of interest, hereby referred to as the working sample, in the path of a collimated beam of light. Samples must have at least a small degree of transparency. The light passes through the working sample and is partially absorbed at characteristic wavelengths corresponding to electronic transitions in the sample. A spectrometer collects the transmitted light and compares the output against a baseline reference measurement corresponding to l 00% T (or 0 A). The reference measurement must consider the absorbance by any material support, such as a cuvette holder or a glass slide. Transmission reference measurements can be accomplished using either a single or double-beam setup.

In a single-beam spectrometer, shown in Figure 2, the user places the reference sample (e.g., an empty cuvette or a clean support free of the absorber material of interest) in the path of the beam and performs a baseline scan. Afterward, the user replaces the reference sample with the working sample for measurement. The drawback to this method is the potential for drift and other fluctuations in the beam to occur over time, especially during warm up. Therefore, it is best to perform a reference scan immediately prior to performing the scan on the working sample to minimize time for beam drift that.

In a two-beam transmission configuration, as shown in Figure 3, the incidence

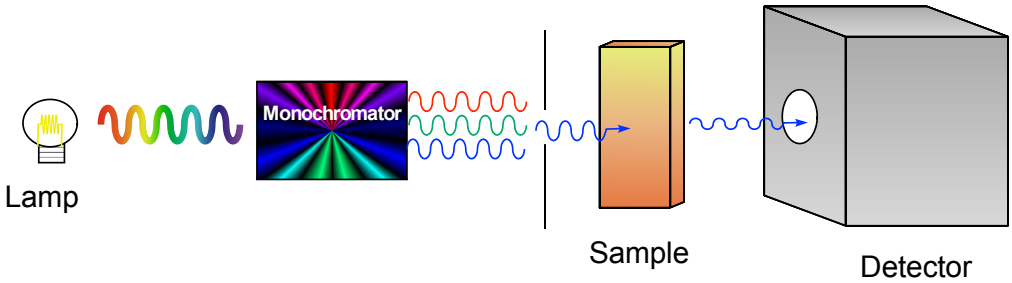

Figure 2 Single beam UV-vis transmission configuration.

beam is split into two paths. The user places the reference sample in one path and the working sample in the other. The spectrometer measures the transmitted light from both samples simultaneously and compares the transmission of the working sample versus the reference, thereby maintaining a dynamic baseline. This may improve reliability in the data by removing any potential for beam drift over time.

Some spectrometers also have dark scan capability. This enables the instrument to account for stray light from the ambient environment that may enter the sampling chamber. The spectrometer collects the dark scan by shuttering the incidence beam and measuring stray illumination that may be present in the chamber. It then subtracts the values obtained in this measurement from scans of the reference and working samples to further improve accuracy. Although this feature is helpful, it does not account for any temporal variations of stray light during measurement, and users should take care to minimize the stray illumination in the detection chamber.

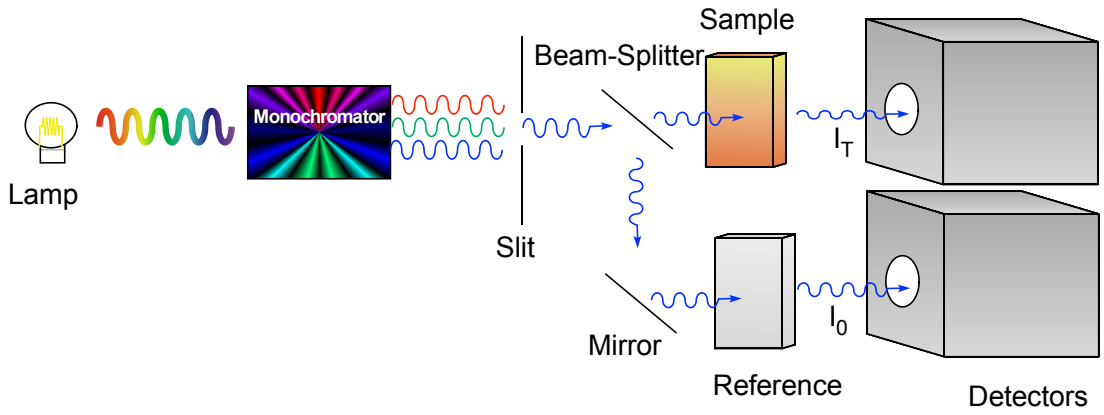

Figure 3 Split dual-beam UV-vis transmission configuration.

Section 3.4: UV-vis Integrating Sphere Spectrometers

In a reflectance configuration, the spectrometer measures the reflected light, rather than the transmitted light, from a sample.

$$R = \frac{I_R}{I_0} \tag{1.6}$$

where I_R is the reflected intensity of the light. Two types of reflection can occur: specular and diffuse. Specular reflection occurs when the incident beam of radiation strikes a flat mirror like sample and reflects from the surface at an angle equal to the angle of incidence. Diffuse reflectance occurs from of mat surfaces when the incident beam penetrates the sample surface, is partially absorbed, and a fraction of its photons is reemitted (reflected) at various angles, Figure 4.

A typical single-beam integrating sphere, Figure 5, has an input port connected to the light source, an output port connected to a detector and an aperture against which the working or reference samples can be placed for measurement. A monochromator is placed either before or after the integrating sphere. The inside of an integrating sphere is covered with a highly reflective material such as polytetrafluoroethylene (PTFE) or Ba_2S0_4, which are reflective over a large wavelength region of interest. This material also serves as a nearly ideal Lambertian scatterer it distributes the light uniformly throughout the entire integrating sphere. A specular reflectance plug can be used to block the specular component of the reflectance. The spectrometer can again be either a double or single bean spectrometer. In the single beam setup, the reference and sample scans are performed sequentially,

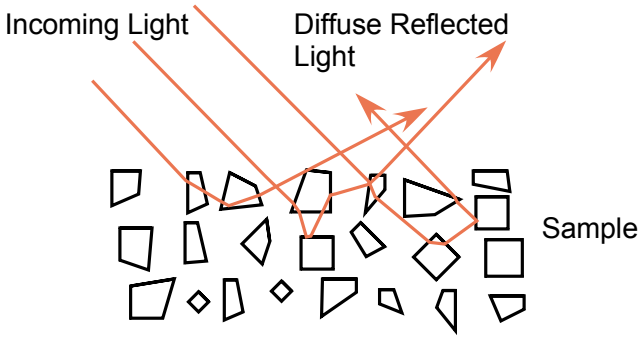

Figure 4 Diffuse reflecting sample.

A double beam integrating sphere spectrometer is shown in Figure 6. In a double beam instrument, the light beam is split by a rotating mirror that alternately reflects the

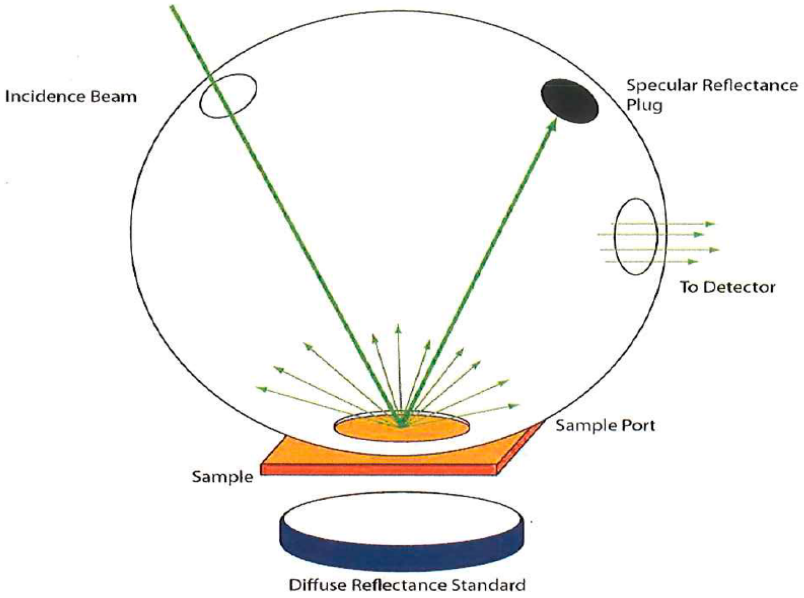

Figure 5 Diffuse reflectance configuration using an integrating sphere with a specular reflectance plug. A diffuse reflectance standard can be placed against a transmissive sample.

light beam to one of the two ports of the integrating sphere. The detector alternately observes light that was reflected from the sample, I_R, or a standard, I_0. The instrument then ratios the two signals. In a double beam setup, the reference and sample scans are performed in parallel.

During diffuse reflectance measurements, specular reflectance will increase noise, decrease the accuracy of the measurement, and can contribute to spurious peaks in the

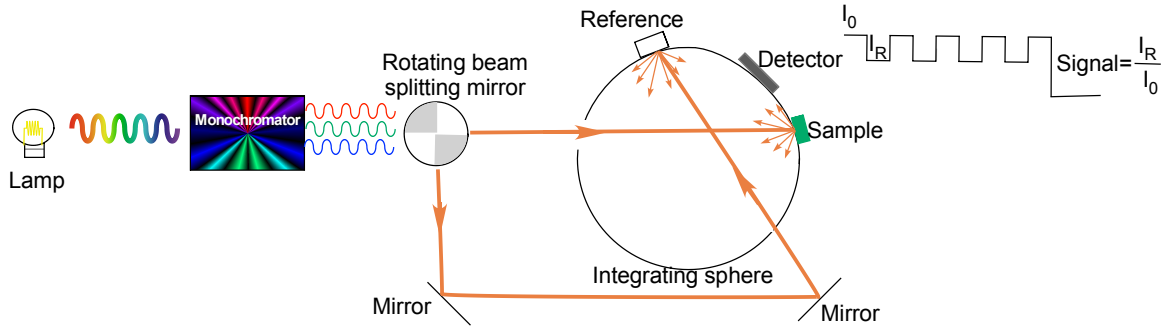

Figure 6 Double beam reflectance spectrometer.

data. Therefore, the specular reflectance needs to be minimized during a measurement. An integrating sphere can contain a specular reflectance sink (or "plug") that minimizes this contribution. For powders, dilution in a non-absorbing matrix can further increase diffuse reflectance while minimizing specular reflectance. Typical non-absorbing matrix materials include KBr, KCI, and Ba_2S0_4 .

In an integrating sphere, three types of measurements are possible. The sample can be placed at the entrance slit of the integrating sphere to measure the transmittance of the sample, placed at the "exit" slit as shown in Figures 5 and 6 to measure the reflectance, or placed in the center of the integrating sphere to measure both the transmittance plus reflectance. When all the reflectance is from the surface of sample (specular) and there is little diffuse reflectance the absorptance, f_A reflectance and transmission are related by

$$f_A + T + R = 1 \qquad 1.7$$

Note that this implies that $I_{abs} = I_0 - I_T - I_R$ and eq 1.5 is not correct. Normally I_R is only a few % of I_0 and can be ignored.

Section 3.5: Diffuse Reflectance measurements

Samples amenable to this configuration include powders or semiconductor films unsupported or supported on reflective or transparent substrates. Substrates that absorb more light than the semiconductor itself, for instance graphite, are not recommended for this configuration as their optical absorption may dominate the measured spectrum. A typical configuration for a reflectance measurement often involves the use of an integrating sphere to capture all photons reflected from the sample, as shown in Figure 5 and 6.

A diffuse reflectance measurement must consider how the sample is mounted to choose a reflectance standard to use for the 100% reflectance or reference scan. The reflectance standard is placed against the exit aperture, or sampling port, of the integrating sphere and the spectrometer collects a baseline, which is used as the reference "spectrum" for 100% transmission. For samples deposited on reflective substrates, such as a metal, the bare metal may serve as the reference or reflectance standard.

Samples deposited onto transparent substrates, such as a transparent conducting oxide on glass (e .g. indium-tin oxide, or ITO), require the use of a white diffuse reflectance standard. This standard is often made from Ba_2S0_4 or PTFE-based material (the same materials as used to coat the interior surface of the integrating sphere). However, the transparent support may have a small absorbance or reflectivity in the region of interest. For these samples, it is advisable to use a bare support (having no absorbing material of interest) with the reflectance standard. The bare support is mounted between the aperture and the reflectance standard at the exit port of the integrating sphere.

Dark scans to calibrate the 0 % reflectance, i.e., complete absorption of the light by the sample, may be simulated by shuttering the light source temporarily.

Following the reference and dark scans; the working sample is placed against the aperture of the integrating sphere. For samples on transparent supports, the diffuse reflectance standard is placed against the backside of the support to reflect any transmitted light back through the sample and into the sphere. The spectrometer then determines the amount of light reflected by the sample by comparison against the reference standard.

In diffuse reflectance measurements, the measured reflectance R is not directly proportional to the absorption coefficient, α; rather a model must be employed to extract something proportional to α. One commonly used model is the Kubeika-Munk radiative transfer model where[4, 5, 16]

$$f(R) = \frac{(1-R)^2}{2R} = \frac{\alpha}{S} \tag{1.8}$$

where $f(R)$ is the Kubeika-Munk function and S is the scattering coefficient. If the scattering coefficient is assumed to be wavelength independent, then $f(R)$ is proportional to α. The assumption of wavelength independency for S can lead to errors. Note that there is significant criticism of the Kubeika-Munk formalism and in many situations the transformed data, $f(R)$, is not linearly proportional to the absorption coefficient. A more rigorous analysis of obtaining the absorption coefficient from diffuse reflectance is described by Murphy.[21, 22]

Section 4: Analysis of Band Gap Energies from UV-vis Spectra

An ideal UV-vis spectrum for a perfect direct band gap semiconductor exhibits almost no absorption for photons with energies below the band gap and a sharp increase in absorption for photons above the band gap. Since spectra are typically reported in units corresponding to the wavelength of light rather than its energy, the conversion between wavelength (nm) and band gap energy (eV) units is achieved by:

$$h\nu\ (\text{eV}) = \frac{hc}{\lambda} = \frac{1239.8\ (\text{eV} \times \text{nm})}{\lambda\ (\text{nm})} \tag{1.9}$$

The band gap in the absorption spectrum corresponds to the point at which absorption begins to increase from the baseline, since this indicates the minimum amount of energy required for a photon to excite an electron across the band gap and thus be absorbed in the semiconductor material. Real spectra exhibit a nonlinear increase in absorption that reflects the local density of states at the conduction band minimum and valence band maximum, as well as excitonic effects.[5]

In a transmission experiment, the instrument software will usually use Equation 1.2 to obtain the absorbance from the measured intensity. However, the measured intensity is affected not only by absorbance, but by reflectance and scattering as well. These effects are often related to the morphology of each sample (e.g., a sample with a rough surface will introduce significant light scattering that decreases the amount of light reaching the detector and cons1.ently increases the perceived absorbance). These effects are often manifested in the form of a non-zero baseline. One way to correct for these effects is to shift all the data so that the data point with the lowest absorbance value corresponds to zero absorbance. This method assumes that any reflectance and scattering effects are wavelength-independent (or if later a sloping baseline is used to correct error that is linear in photon energy). It is important to realize that this assumption is not always valid and can introduce error in the data analysis. A detailed band gap analysis involves plotting and fitting the absorption data to the expected trend lines for direct and indirect band gap semiconductors. The absorbance A is first normalized to the path length l of the light through the material to produce the absorption coefficient, α, as per Equation 1.3. Values of a > 10^4 cm^{-1} often obey the following relation presented by Tauc and supplied by Davis and Mott[2, 3]

$$\alpha h\nu \propto (h\nu - Eg)^n \tag{1.10}$$

where n can take on values of 3, 2, 3/2, or 1/2, corresponding to indirect (forbidden), indirect(allowed), direct (forbidden), and direct (allowed) transitions, respectively.[1, 6-8] These so-called Tauc plots[9-11] of ($\alpha h\nu$)^n vs. $h\nu$ yield the value of the band gap when extrapolated to the baseline are summarized in Table 1.

Table 1 Tauc plots and their respective transition types.

Plot	Transition
$(\alpha h\nu)^2$ vs $h\nu$	Direct (allowed)
$(\alpha h\nu)^{2/3}$ vs $h\nu$	Direct (forbidden)
$(\alpha h\nu)^{1/2}$ vs $h\nu$	Indirect (allowed)
$(\alpha h\nu)^{1/3}$ vs $h\nu$	Indirect (forbidden)

For values of α < 10^4 cm^{-1}, an exponential tail often exists for many materials that cannot be modeled by Equation 1.9-10. [2, 3, 5, 12-14] The value of

10^4 cm^{-1} is not a strict cutoff and will vary from one system to another. The Kubeika-Munk function discussed above gives

$$f(R)=\frac{\left(1-R\right)^2}{2R}=\frac{\alpha}{S} \tag{1.8}$$

If the scattering coefficient is assumed to be wavelength independent, then $f(R)$ is proportional to α and the Tauc plots can be made using $f(R)$ in place of α[17-20]. However, since it is not possible to accurately plot the value of α without knowing the scattering coefficient, care must be taken to extrapolate the band gap from higher values of $f(R)$. Extrapolation from the region of the exponential tail can lead to underestimation, as noted above. A more rigorous analysis of obtaining the absorption coefficient from diffuse reflectance is described by Murphy.[21, 22]

To estimate the nature and value of the band gap, the experimentally derived absorption curve can be plotted according to Table 1. As an example, the absorbance of an electrodeposited polycrystalline Cu_20 sample measured using a transmission configuration and shown in Figure 7. The absorbance data was first shifted such that the lowest value was set to zero to account for any wavelength-independent reflectance and scattering. The absorbance was then analyzed using Equation 1.3 for its absorption coefficient in Figure 7 (a) and in the form of Tauc plots in (b-d). For plots (c-e), a tangent is first drawn to the baseline at low energies-in this case, from 1.3 – 2.0 eV. This step may not be necessary for plots that have little to no baseline, as is often the case with direct (allowed) band gap and shown in Tauc plots such as plot (b). This accounts for light that reaches the spectrometer due to a wavelength dependent reflection or scattering processes not accounted for by the reference standard as well as from multiplication of α by increasing values of $h\nu$. A linear baseline only accounts for reflections or scattering that are linear dependence with photon energies, and cannot take into account nonlinear effects (e.g., Rayleigh, Mie, plasmonic etc. scattering). Cu_20 also has contributions to its baseline from an absorption tail apparent in plots (c-e) that has previously been attributed to absorption from copper ion vacancies and free carriers.[23-25] Second, a line tangent to

the slope in the linear region of the absorption onset is drawn. The intersection of the two lines corresponds to the best estimate for the energy of the band gap.

Plot (b) shows that this particular Cu_20 sample has an allowed direct band gap near 2.4 eV, while plots (c-e) show another transition near 2.0 eV that could be attributed to any of the three other transitions listed in Table 1. This example illustrates that while Tauc plots provide a formal procedure for analyzing absorption data, they do not necessarily provide a conclusive assessment of the band gap nature, which perhaps explains the range of reports in literature for Cu_20. Thus, it is good practice and helpful to readers to show unprocessed UV-vis absorption data for a given material in the form of an absorption coefficient vs. energy plot such as in Figure 7 a to provide insight as to the photon energy at which absorption onset occurs.

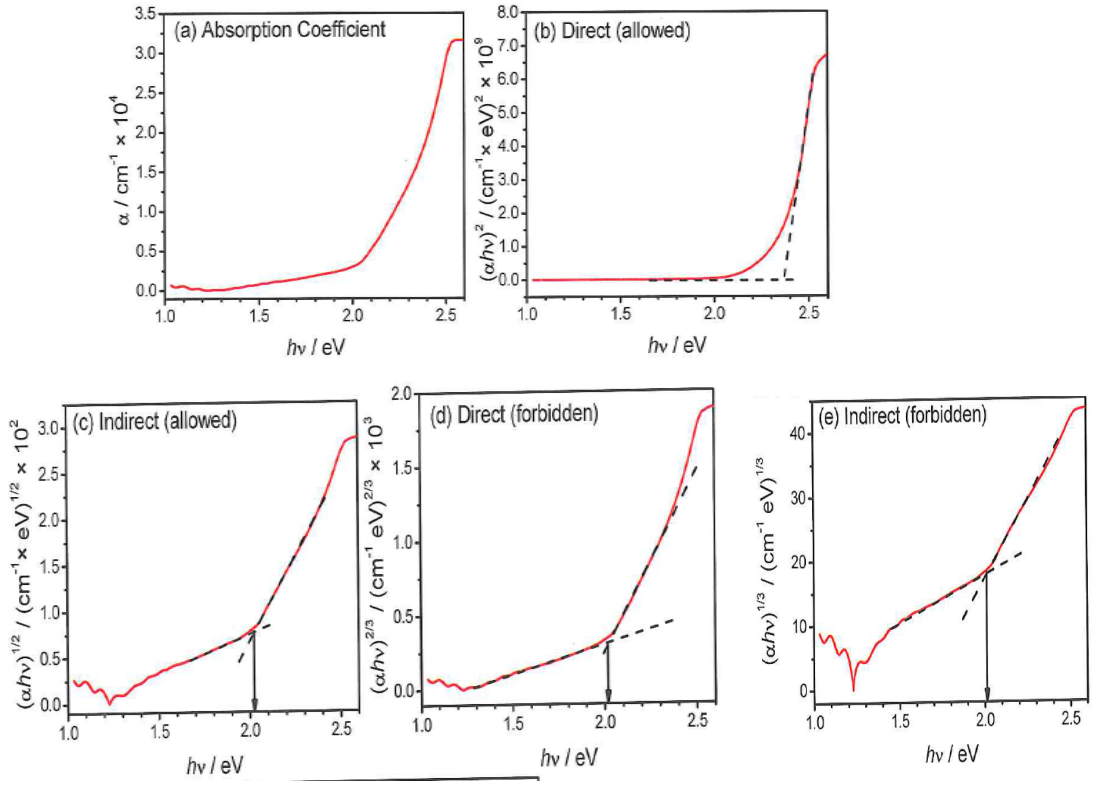

Figure 7 (a) Absorption data from a 1.7 µm film of electrodeposited polycrystalline Cu20 plotted in (b) allowed, (c) allowed indirect, (d) forbidden direct, and (e) forbidden indirect band gap Tauc plots. Plot (b) suggests an allowed direct transition with a band gap of approximately 2.4 eV, consistent with previous reports.[26-29] Plots (c-e) suggest transitions near 2.0 eV, but do not conclusively indicate the nature of the transition. Cu20 literature supports both allowed indirect[30, 31] and forbidden direct[32, 33] transitions. Allowed direct transitions near 2.0 eV have also been observed.[34, 36] An absorption tail below 2.0 eV that has previously been attributed to copper ion vacancies and free carriers.[23, 25]

In general, a UV-vis transmission experiment offers the fastest and most direct method of estimating the optical bulk band gap and should be a priority for any newly synthesized material. A diffuse reflectance configuration can be used if the sample is not transmissive. If a diffuse reflectance experiment is not available, then photocurrent spectroscopy (as described in the Photocurrent Onset document) with extremely facile redox couples can be performed, though errors in this method may arise from poor charge carrier mobilities or lifetimes and from slow kinetics at the sample-electrolyte interface.

Section 5: Equipment for UV-vis Measurements

Commercial UV-vis spectrometers are widely available in both transmission and diffuse reflectance configurations. These machines often offer an extremely wide wavelength window over which measurements can be performed, extending from the UV to the NIR regions.

A modular setup can be assembled in a laboratory for cost reduction purposes or for additional flexibility. At a minimum, the required equipment includes:

- Light source
- Monochromator with detector or polychromator with detector array
- Long pass filters
- Transmission cell
- Diffuse reflectance sphere
- Various focusing lenses and optical fibers

Items of note are the types of light sources and the long pass filters. The light source can come in the form of arc lamps (mercury, tungsten-halogen, xenon) or tunable dye lasers. Care must be taken to maintain sample integrity during broad spectral range illumination. For example, xenon lamps produce large intensity in the infrared spectral region, which can locally heat and possibly damage a sample if an infrared absorbing filter (such as a water column) is not used.

The choice of lamp is often dictated by the wavelength range desired for a given experiment. For work that primarily requires a large amount of UV radiation in the range of 160-400 nm, deuterium lamps are preferable. For larger ranges of 200-2500 nm,

xenon and mercury lamps will be necessary. Many off-the-shelf instruments contain multiple lamps to adequately cover the full spectrum of interest.

Long pass filters eliminate spurious bands that arise from harmonics in the separation of light in the monochromator. For example, if the monochromator is set to output light with a wavelength of 700 nm, light at wavelengths of 350 and 175 nm will also be emitted. Therefore, a long pass filter that eliminates light below 400 nm would be required to properly control the output of the monochromator.

Diffuse reflectance integrating spheres are commercially available from multiple vendors. For a given light input, a smaller sphere will be brighter than a larger sphere since the internal surface area is smaller. However, light throughput can be negatively affected if a sphere is too small, since the presence of input, output, and sampling ports distort the ideal spherical geometry and decrease the hemispherical reflectance. Many integrating spheres have an optimum diameter of 2-4 inches with area of the ports making up 5% or less of the total internal surface area[4].

Section 5. References

1. S. M. Sze and K. K . Ng: Physics of Semiconductor Devices (2006).

2. D. L. Wood and J. Tauc: Weak Absorption Tails in Amorphous Semiconductors. Physical Review B 5, (**1972**), 3144

3. E. A. Davis and N. F. Mott: Conduction in non-crystalline systems V. Conductivity, optical absorption, and photoconductivity in amorphous semiconductors. Philosophical Magazine 22, (**1970**), 0903.

4. Integrating Spheres - Introduction and Theory. Comprehensive Catalog of FTIR Accessories and Supplies, Pike Technologies (**2005**) https://www.google.com/search?client=safari&rls=en&q=4.+Integrating+Spheres+-+Introduction+and+Theory.+Comprehensive+Catalog+of+FTIRAccessories+and+Supplies+(2005).&ie=UTF-8&oe=UTF-8.

5. J. D. Dow and D. Redfield: Electroabsorption in Semiconductors: The Excitonic Absorption Edge. Physical Review B 1, (**1970**).

6. M. Anwar and C. A. Hogarth: Optical Prope1ties of Amorphous Thin Films of $Mo0_3$ Deposited by Vacuum Evaporation. Physica Status Solidi 109, (**1988**).

7. K. Santra, C. K. Sarkar, M. K. Mukhejee and B. Ghosh: Copper oxide thin films grown by plasma evaporation method. Thin Solid Films 213, (**1992**).

8. F. P. Koffyberg, K. Dwight and A. Wold: Interband Transitions of Semiconducting Oxides Determined from Photoelectrolysis Spectra. Solid State Communications 30, (**1979**).
9. R. J. Elliott: Intensity of optical absorption by excitons. Physical Review 108, (**1957**).
10. J. Tauc, R. Grigorovici, and A. Vancu: Optical properties and electronic structure of amorphous germanium. J Phys. Soc. Jpn. 21, (**1966**), 627.
11. J. Tauc, A. Menth and D. L. Wood: Optical and magnetic investigations of localized states in semiconducting glasses. Phys. Rev. Lett. 25, (**1970**), 749.
12. F. Urbach: The Long-Wavelength Edge of Photographic Sensitivity and of the Electronic Absorption of Solids. Physical Review 92, (**1953**).
13. R. A. Street and N. F. Mott: States in the Gap in Glassy Semiconductors. Physical Review Letters 35, (**1975**).
14. J. Tauc, A. Menth and D. L. Wood: Optical and Magnetic Investigations of the Localized States in Semiconducting Glasses. Physical Review Letters 25, (**1970**).
15. Y. I. Kim, S. J. Atherton, E. S. Brigham and T. E. Mallouk: Sensitized layered metal oxide semiconductor pa1ticles for photochemical hydrogen evolution from nonsacrificial electron donors. The Journal of Physical Chemistry 97, (**1993**).
16. P. Kubeika: New Contributions to the Optics of Intensely Light-Scattering Materials. PattI. Journal of the Optical Society of America 38, (**1948**).
17. A. P. Finlayson, V. N. Tsaneva, L. Lyons, M. Clark and B. A. Glowacki: Evaluation of BiW-oxides for visible light photocatalysis. Physica Status Solidi 203, (**2006**).
18. N. Kislov, S.S. Srinivasan, Y. Emirov and E. K. Stefanakos: Optical absorption red and blue shifts in $ZnFe_20_4$ nanoparticles. Materials Science and Engineering B 153, (**2008**).
19. E. S. Brigham, C. S. Weisbecker, W. E. Rudzinski and T. E. Mallouk: Stabilization of Intra Zeolitic Cadmium Telluride Nanoclusters by Ion Exchange. Chemistry of Materials 8, (**1996**).
20. D. G. Ba1ton, M. Shtein, R. D. Wilson, S. L. Soled and E. Iglesia: Structure and Electronic Properties of Solid Acids Based on Tungsten Oxide Nanostructures. The Journal of Physical Chemistry B 103, (**1999**).
21. A. B. Murphy: Band-gap determination from diffuse reflectance measurements of semiconductor films, and application to photoelectrochemical water-splitting. Solar Energy Materials & Solar Cells 91, (**2007**), 1326.
22. A. B. Murphy: Optical properties of an optically rough coating from inversion of diffuse reflectance measurements. Applied Optics 46, (**2007**).
23. V. F. Drobny and D. L. Pulfrey: Prope1ties of reactively-sputtered copper-oxide thin films. Thin Solid Films 61, (**1979**).
24. A . E. Rakhshani and J. Varghese: Optical-absorption coefficient and thickness measurement of electrodeposited films of Cu_20. Phys. Status Solidi A-Appl. Res. 101,(**1987**).

25. H. Wieder and A. W. Czanderna: Optical properties of copper oxide films. J. Appl. Phys.37, (**1966**).

26. X. Mathew, N. R. Mathews, and P. J. Sebastian: Temperature dependence of the optical transitions in electrodeposited Cu_20 thin films. Sol. Energy Mater. Sol. Cells 70, (**2001**).

27. B. Balamurugan, B. R. Mehta, D. K. Avasthi, F. Singh, A. K. Arora, M. Rajalakshmi, G.Raghavan, A. K. Tyagi and S. M. Shivaprasad: Modifying the nanocrystalline characteristics – structure, size, and surface states of copper oxide thin films by high energy heavy-ion irradiation. J. Appl. Phys. 92, (**2002**).

28. J. F. Pierson, A. Thobor-Keck, and A. Billiard: Cuprite, paramelaconite and tenorite films deposited by reactive magnetron sputtering. Appl. Surf Sci. 210, (**2003**).

29. N. A. M. Shanid and M. A. Khadar: Evolution of nanostructure, phase transition and band gap tailoring in oxidized Cu thin films. Thin Solid Films 516, (**2008**).

30. T. Kosugi and S. Kaneko: Novel spray-pyrolysis deposition of cuprous oxide thin films. J. Am. Ceram. Soc. 81, (**1998**).

31. A. E. Rakhshani: Preparation, characteristics, and photovoltaic properties of cuprous oxide - a review. Solid-State Electron. 29, (**1986**).

32. K. Santra, C. K. Sarkar, M. K. Mukherjee, and B. Ghosh: Copper-oxide thin-films grown by plasma evaporation method. Thin Solid Films 213, (**1992**), 226.

33. P. E. de Jongh, D. Vanmaekelbergh and J. J. Kelly: Cu_20: Electrodeposition and characterization. Chem. Mat. 11, (**1999**), 3512.

34. A. S. Reddy, G. V. Rao, S. Uthanna and P. S. Reddy: Structural and optical studies on reactive magnetron sputtered Cu_20 films. Mater. Lett. 60, (**2006**).

35. T. Mahalingam, J. S. P. Chitra, J.P. Chu, H. Moon, H.J. Kwon and Y. D. Kim: Photoelectrochemical solar cell studies on electroplated cuprous oxide thin films. J. Mater. Sci. -Mater. Electron. 17, (**2006**), 519.

36. W. Siripala, L. Perera, K. T. L. DeSilva, J. Jayanetti and I. M. Dharmadasa: Study of annealing effects of cuprous oxide grown by electrodeposition technique. Sol. Energy Mater. Sol. Cells 44, (**1996**), 251.